Hindawi
Advances in Materials Science and Engineering
Volume 2020, Article ID 6729754, 9 pages
https://doi.org/10.1155/2020/6729754

Research Article

The Effect of Network Structure on Compressive Fatigue Behavior of Unfilled Styrene-Butadiene Rubber

Liu Yang, Kaikai Liu, and Aihua Du

Key Lab of Rubber-plastics, Ministry of Education, Qingdao University of Science & Technology, Qingdao 266042, China

Correspondence should be addressed to Aihua Du; aihuadu@qust.edu.cn

Received 15 November 2019; Revised 17 February 2020; Accepted 24 February 2020; Published 17 April 2020

Academic Editor: Marino Lavorgna

The effect of network structure on dynamic compressive fatigue behavior and static compressive mechanical properties of styrene-butadiene rubber (SBR) were investigated. A series of SBR compounds with different amounts of sulfur and dicumyl peroxide (DCP) were prepared, and their crosslinking densities were calculated using the Flory–Rehner equation. Compressive fatigue resistance and creep behavior of the vulcanizates were performed on a mechanical testing and simulation (MTS) machine. The fatigue damage surface of SBR vulcanizates before and after a dynamic compressive fatigue test was observed with a scanning electron microscopy (SEM). The results suggested that the surface of the samples was badly damaged as the number of compressive cycles increased. By comparison, compressive fatigue caused less surface damage to sulfur-cured SBR than to peroxide-cured SBR. The peroxide-cured SBR samples showed higher energy dissipation than sulfur-cured SBR during cyclic compression. The peroxide-cured SBR showed lower creep strain and compression set than the sulfur-cured SBR. The -Sx- linkages provided by the sulfur curing system allow dynamic compressive deformation but suffer from poor static compressive resistance. However, the carbon-carbon linkages from DCP are irreversible and provide higher resistance to static compressive stress, but they do not show obvious dynamic compressive fatigue resistance.

1. Introduction

Rubber materials are widely used in industrial fields because of their high elasticity and excellent damping properties [1, 2]. However, fatigue failures that are common in rubber components remain a key issue. Rubber components, such as seals, tires, and automotive mounts, are usually subjected to static or dynamic compressive loading environments in service life. Such rubber materials may fail due to cyclic loading. The damage surface shows as millimeter-sized voids in the contact surfaces [3–9]. The compressive fatigue damage process of rubber materials is complex, affected by many factors, and is still not completely understood. Cyclic compressive deformation is one of the causes of fatigue damage in rubber components which causes small voids and cracks that propagate to eventual failure [10].

Some researchers [11–15] have studied the fatigue behavior of rubber materials under cyclic tension loading conditions. Up to now, only several studies study the fatigue behaviors of SBR under compression loading conditions with different crosslink network structures [16–18]. Le Cam et al. [19] described fatigue behavior in natural rubber filled with carbon black under tension-compression conditions. Seichter et al. [14] studied the effect of frequency on the fatigue behavior of SBR/NR/BR blends under uniaxial loading. Wu [20] studied the compression fatigue behavior of compound concrete and discussed the changes in the dissipated energy, Poisson's ratio, residual strain, and fatigue modulus of the cylindrical samples with the number of compressive cycles. Wu [21] studied the stress-strain response and mechanical properties of SBR/NR vulcanized rubber fenders under static and dynamic compressive conditions.

Rubber compounds are crosslinked by the curing system. The sulfur and peroxide are the two commonly used curing system. Sulfur is commonly used in rubber compounds in amounts of 1–3 phr. Sulfur curing system produces polysulfidic, disulfidic, and monosulfidic crosslink.

The former is good for fatigue resistance. Carbon-carbon crosslinks are commonly introduced by peroxide curing system into vulcanizates to improve static mechanical performance. The type of crosslink bonds and crosslinking densities will determine the properties of vulcanizates under static and dynamic loading conditions [22]. Thus, the study of the effect of network structure on fatigue behavior of rubber is of major importance to extend the service life. Fu et al. [23] investigated the influence of the network structure on the mechanical properties and fatigue life of natural rubber. It was found that the presence of the weak bonds in the crosslink network provides higher toughness and tensile strength, thereby further extending the fatigue life of natural rubber.

Our work focuses on styrene-butadiene rubber (SBR) composites cured by peroxide-cured systems and sulfur systems to investigate the effect of network structure on the compressive fatigue behavior of unfilled styrene-butadiene rubber. The compressive fatigue behavior of unfilled SBR in the dynamic conditions was correlated with the polymer crosslink network structure. The dynamic and static compressive fatigue behavior was investigated by characterizing their hysteresis loops, dissipated energy, S-N curves, damage surface morphology, compression set, and creep behavior. We attempted to obtain a better understanding of the influence of network structure on the compressive fatigue behavior of unfilled SBR vulcanizates.

2. Experimental

2.1. Materials and Basic Formulation. Formulations of SBR are shown in Table 1, where S-SBR and DCP-SBR represent the sulfur- and DCP-cured SBR, respectively. Nos. 1–5# represent the dosage of curing agent (1, 1.5, 2, 2.5, and 3 phr).

Styrene-butadiene rubber (ESBR 1502) was acquired from Sinopec Qilu Company Ltd; other additives, such as dicumyl peroxide (DCP), sulfur (S), zinc oxide (ZnO), stearic acid (SA), accelerator N-tert-butylbenzothiazole-2-sulphenamide (NS), and antiaging agent N-isopropyl-N′-phenyl-p-phenylenediamine (4010 NA), were industrial-grade products.

All the compounds given in Table 1 were masticated on a two-roll laboratory mill. Vulcanization was carried out at 160°C (for S-SBR) and 170°C (for DCP-SBR) with a pressure of 10 MPa, according to the optimum curing time determined by the vulkameter (GT-M2000-A cure meter from Gaotie Science and Technology Company, Taiwan, China).

2.2. Tests and Analysis. The crosslinking densities of vulcanizates were determined by the Flory–Rehner equation shown in equation (1). To achieve their swollen equilibrium, weighed samples were, respectively, immersed in toluene at room temperature for 72 hours. The toluene was changed every 24 hours to ensure that all uncrosslinked rubber materials were removed. The swollen samples were dried after 72 hours, and the crosslinking density (V_e) was calculated using the following equation:

Table 1: Formulations in parts per hundred rubber (phr).

Ingredients	Quantity	
	S-SBR	DCP-SBR
SBR	100	100
ZnO	5	5
SA	2	2
4010 NA	2	2
NS	1	—
S	Variable (1, 1.5, 2, 2.5, 3)	—
DCP	—	Variable (1, 1.5, 2, 2.5, 3)

$$V_e = -\frac{\ln(1 - V_r) + V_r + \chi V_r^2}{V_1\left(V_r^{1/3} - 1/2V_r\right)}, \quad (1)$$

where V_1 is the molar volume of solvent, V_r is the volume fraction of rubber in the swollen sample, and $\chi = 0.446$ represents the Flory–Huggins rubber-solvent interaction term.

Compression set was tested by the following steps. Three cylindrical samples with dimensions $12.5 * 29 * 29$ mm were compressed 25% for 72 hours. Then, the samples were relaxed at room temperature for 30 min. After that, the recovered height of cylindrical samples was recorded and the compression value (C_d) was determined using the following equation:

$$C_d = \frac{H_0 - H_f}{H_0 - H_s} \times 100, \quad (2)$$

where H_0 is the original height of the cylindrical sample, H_s is the compressed height (25% of H_0), and H_f is the final height of the sample.

Compressive fatigue behavior of the vulcanizates was performed on an MTS machine. The shape and size of the testing sample are the same as those of the compression set sample ($12.5 * 29^2$ mm). The dynamic compressive fatigue tests were carried out on an amplitude of 3.75 mm at 10 Hz using a sinusoidal signal. At the beginning of the high-cycle compressive experiment, the samples produced lateral deformation and this kind of deformation gradually became apparent because of the compressive displacement. This is due to the high Poisson's ratio of the rubber materials, as shown in Figure 1(b).

Creep tests were also carried out on this MTS instrument using 1 MPa constant compressive stress and measuring time-dependent deformation.

Changes in the specimen surfaces before and after fatigue were studied using JSM-6700F scanning electron microscope (SEM).

3. Results and Discussion

3.1. Effect of Curing Agent Amounts on the Crosslinking Density of Vulcanizates. Table 2 shows the crosslinking density of the vulcanizates as a function of the amounts of curing agents used. The crosslinking densities of samples showed an ascending trend with the increase of sulfur and DCP. To investigate only the influence of the linkage type,

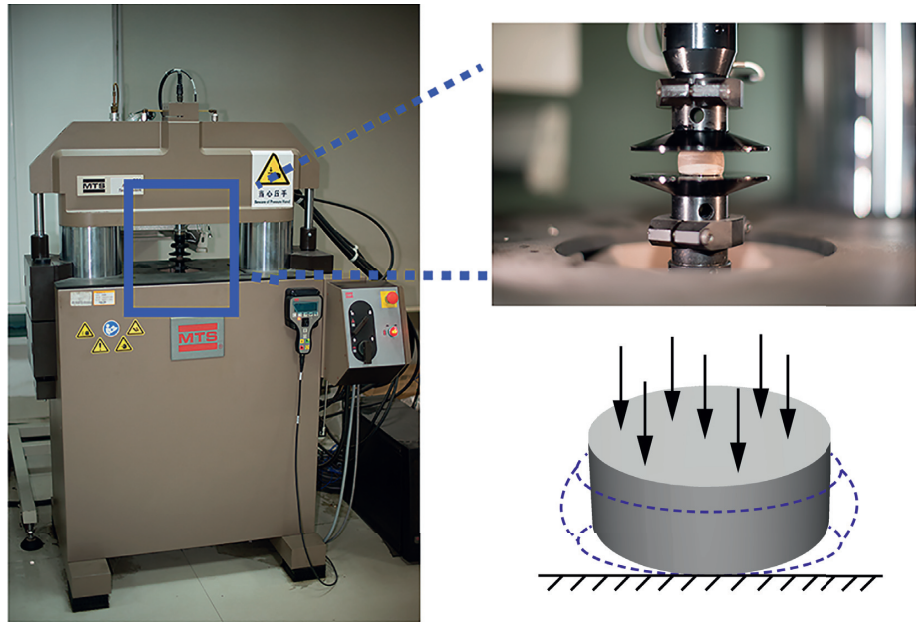

(a) (b)

Figure 1: Testing setup and samples. (a) MTS test system; (b) cylindrical sample under compression.

the crosslinking density of samples must be in the same range for both types of linkage. Therefore, five samples with different crosslinking types but similar crosslinking density (S-SBR 1, DCP-SBR 3, DCP-SBR 4, S-SBR 2, and S-SBR 3) were chosen for comparison.

3.2. Dynamic Compressive Fatigue Behavior. The surface morphology of samples compressed at different cycles and stress-strain relationship for samples S-SBR 2 and DCP-SBR 5 during fatigue cycling are shown in Figure 2. Even if the crosslinking density of the two samples is similar, the fatigue behavior of the two samples is very different. To illustrate the process of surface damage, the high-cycle compression was stopped periodically (every 2000 cycles) and photos of the sample surface were taken. As shown in Figures 2(a) and 2(b), these samples are damaged due to cyclic compression, and the sample surface is badly damaged. For better observation, concentric circles of different colors were drawn on the surface of the samples before the cyclic compression test. The experimental results indicate that the compressive fatigue behavior is significantly affected by the type of linkage. The surface damage of the two samples is more serious as the number of compressive cycles increases. Moreover, cyclic compression caused less surface damage to S-SBR 2 than to DCP-SBR 5 under the same compressive cycles. With the combination of the photos and three-dimensional hysteresis loops in Figures 2(c) and 2(d), the fatigue behavior was explored and correlated with hysteresis to reveal the rubber damage mechanism. The maximum stress decreases greatly during the first several cycles and then stabilizes after several cycles. This phenomenon is known as Mullin's effect. After that, the stress increased progressively. When the stress of the samples decreases to the minimum value, the vulcanizate is regarded as compressive fatigue failure, and the corresponding cycle of failure is considered to be the compressive fatigue life of the SBR (N_f). As shown in Figures 2(a) and 2(b), during the first few thousand cycles, only a small amount of debris and voids appeared on the surface and then the surface began to be damaged gradually. The decrease in stress during the compressive fatigue test is mainly caused by cracks. After approximately N_f cycles, the surface morphology began to change that the debris was gathered in the middle area and gradually became dense, which led to an increase in stress. The minimum stress is observed at about $N_f = 4000$ for S-SBR 2 and $N_f = 1000$ for DCP-SBR 5. Hence, N_f is the transitional phase, in which the hysteresis changed significantly. This correlates very well with Figures 2(a) and 2(b). All tests are performed for at least 10000 cycles to ensure that minimum stress can be observed.

Figures 2(e) and 2(f) show the stress-strain hysteresis loops of S-SBR 2 and DCP-SBR 5 obtained in the 10th and 100th cycles up to the N_f cycles of the cyclic compression test. Dissipated energy E_{diss} is defined as the area of the hysteresis loop and it represents the energy loss during one cycle which is converted into heat. Since this additional thermal load can gradually degrade the rubber, it is important to investigate the dissipated energy. As shown in Figures 2(e) and 2(f), the E_{diss} decreases rapidly at the beginning and then remains stable. Based on the consideration of the different crosslink network structures within the S-SBR 2 and DCP-SBR 5, the hysteresis loop of the DCP-SBR 5 changes more than that of S-SBR 2. This correlates also very well with Figures 2(a) and 2(b); the surface damage of DCP-SBR 5 was worse than that of S-SBR 2. Compared with the sulfur-cured system, the networks of the peroxide-cured SBR were composed of a large amount of C-C crosslink

Table 2: Crosslinking density of vulcanizates.

Sample	S-SBR 1	S-SBR 2	S-SBR 3	S-SBR 4	S-SBR 5	DCP-SBR 1	DCP-SBR 2	DCP-SBR 3	DCP-SBR 4	DCP-SBR 5
Crosslinking density $\times 10^{-4}/cm^3$	3.38 ± 0.11	6.69 ± 0.160.16	7.81 ± 0.06	9.61 ± 0.09	10.93 ± 0.57	2.34 ± 0.090.09	4.00 ± 0.37	4.64 ± 0.14	5.70 ± 0.120.12	6.83 ± 0.230.23

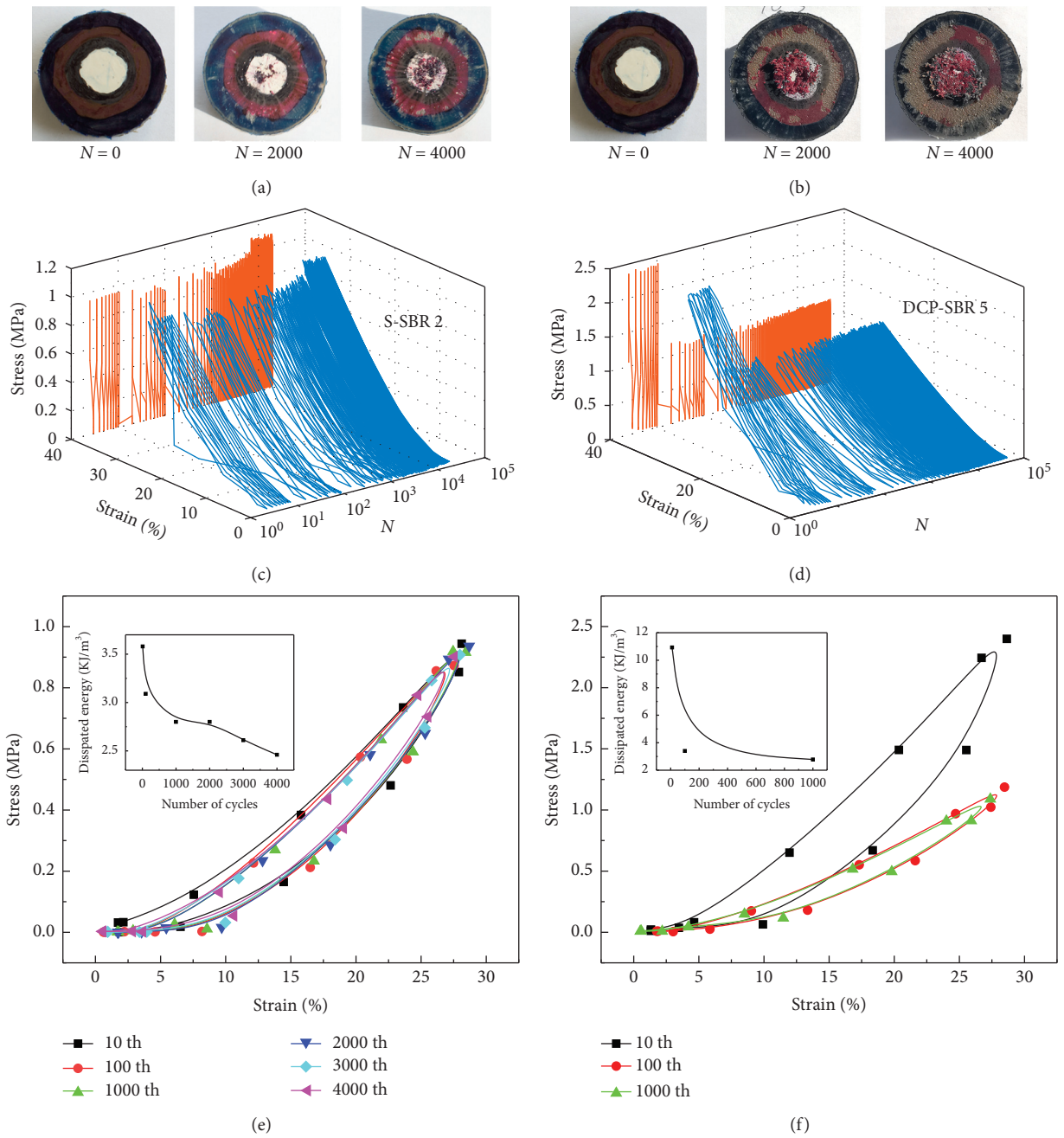

FIGURE 2: (a, b) Top view of damage surfaces of S-SBR 2 sample and DCP-SBR 5 sample after different compressive test cycles, (c, d) three-dimensional compressive stress-strain curves of two samples, and (e, f) stress-strain curves and corresponding dissipated energy of two samples during fatigue cycling.

bonds that have worse chain flexibility than polysulfide bonds. Therefore, its local segment moves slowly. It was considered responsible for the poor dynamic fatigue resistance due to localized stress accumulation.

For the five samples involved in this study, the variations of stress (S) with the applied cycles (N) are shown in Figure 3(a). The results show that the fatigue life of S-SBR samples gradually extends with the increase of sulfur content, while the fatigue life of the DCP-SBR samples decreases with increasing DCP content. Additionally, the N_f data show that the vulcanizates cured with sulfur exhibit longer fatigue life compared with the DCP-SBR samples. It can be attributed to the greater chain flexibility of polysulfide bonds (-S_x-). The -S_x- with greater chain flexibility can deliver higher energy and prolong the compressive fatigue life of vulcanizates. The flexibility of the -Sx- can relieve stress and help to improve the mechanical properties, eventually leading to the good compressive fatigue resistance of SBR. However, carbon-carbon single bonds (C-C) have higher bond energy, which is more rigid, leading to stress

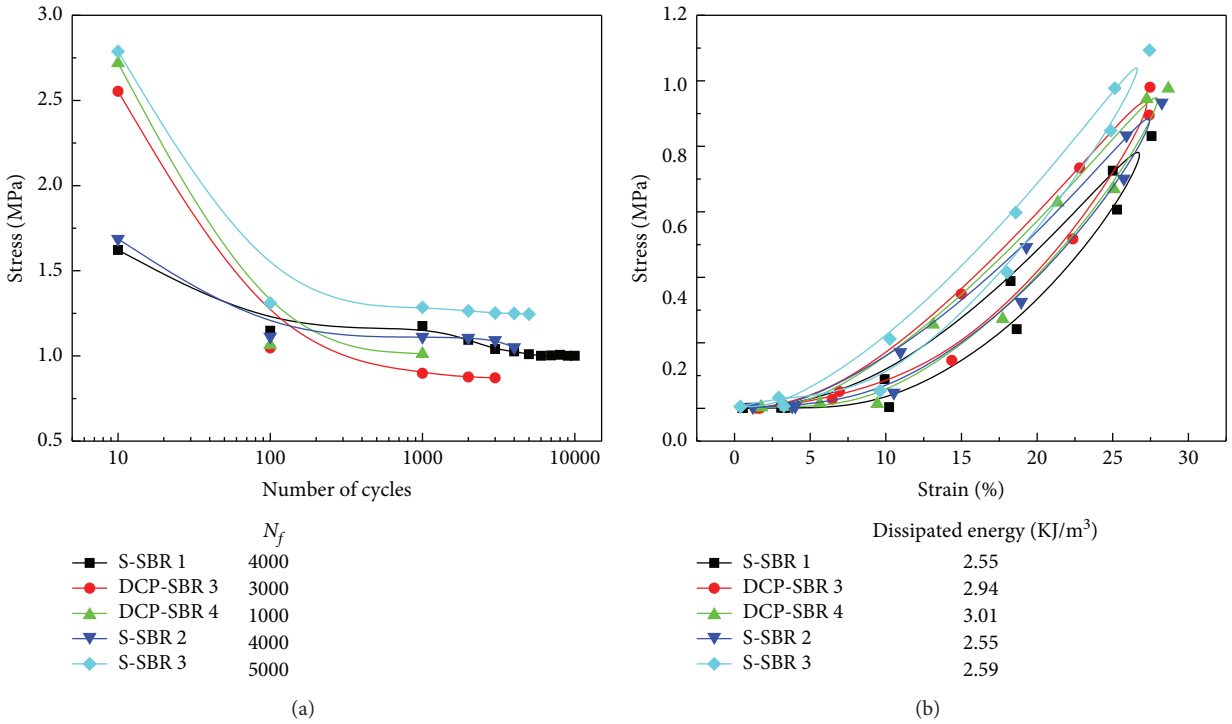

FIGURE 3: S-N curves (a) and dissipated energy (b) of five different samples with the same crosslinking density degree but different types of linkages.

concentration during the compressive cycle. The C-C linkages from DCP-SBR samples are irreversible and provide lower resistance to fatigue.

Figure 3(b) shows the hysteresis loops obtained in the N_f cycles of the five different samples. The E_{diss} increases slightly with increase of crosslinking density. It increases the inner friction of rubber which is provided by the increase in E_{diss}. When the crosslinking densities are similar, the E_{diss} values of the peroxide-cured SBR samples are higher than those of the sulfur-cured SBR. The greater chain flexibility of the -Sx- linkages could offer effective energy delivery to avoid rubber damage. Compared with the S-SBR system, the DCP-SBR samples have higher energy dissipation. As we discussed before, the DCP-SBR samples are more vulnerable to stress concentration, which leads to the breakdown of the crosslink network. The breakage of the -C-C- crosslinks provides high energy loss during deformation. The dissipated energy is transferred into heat, which leads to serious damage to the DCP-SBR samples. From the analysis above, it was concluded that sulfur-cured SBR worked better than peroxide-cured SBR under dynamic compressive conditions. It infers that polysulfide crosslinks are highly resistant to cyclic deformations.

3.3. Surface Damage Characteristics before and after Dynamic Compressive Fatigue. The scanning electron microscopy (SEM) images of the damaged surface are shown in Figure 4. The flat surface was found on the top side of the sample before the compression test. However, for the sample after 10000 cycles of the compressive test, the surface morphology turned rough. At the same time, peeling and voids were formed on the surface. In addition, due to the significantly high amount of granular powder accumulated in the central region, the compact layer was formed on the sample surface as shown in Figure 4(b). Generally, after the compressive fatigue test, there are two main types of damage: peeling and spalling. The peeling usually shows as a wave (Figure 4(c)), while the spalling shows as deeper voids (Figure 4(d)) on the surface.

The mechanism of compressive fatigue behavior was similar to fatigue wear in the early stage. With further cyclic compression, stress concentrated in the center which lead to cracks below the surface and ultimately appeared on the surface. Cracks below the surface led to fatigue wear and formed a large piece of debris and left many voids. As the number of cycles further increases, the wave extends and the number of voids increases. Finally, in Figure 4(b), a compact layer can be observed in the central region.

Figure 5 illustrates a schematic of rubber fatigue damage caused by repeated compressive stress cycles and the crack initiation process. It is obvious from the subsurface deformation of rubber material that the maximum stress will generate cracks and develop below the surface [24, 25]. The small cracks that develop below the surface will then propagate to the free surface and combine with each other because of repeated stress cycles, and finally, rubber damage occurs.

3.4. Monotonic Compressive Behavior. At the same time, we tested the static compression behavior in two modes, i.e.,

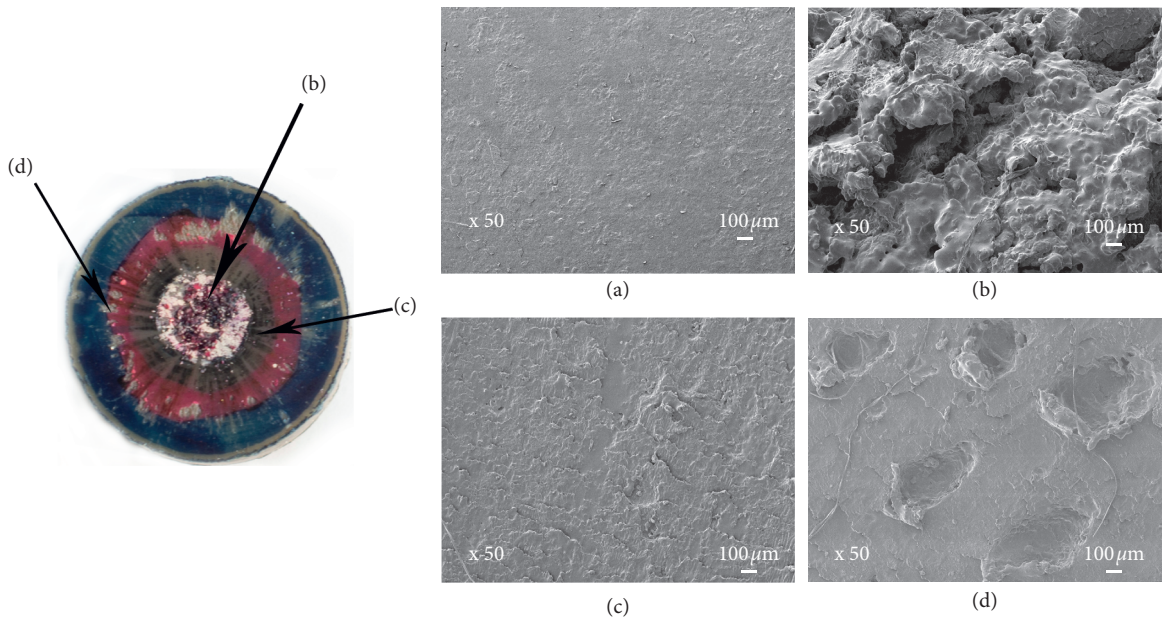

Figure 4: SEM images of surface damages of S-SBR 2 sample before and after 10000 compressive test cycles: (a) before fatigue test, (b) central region after test, (c) showing the wave, and (d) showing the voids.

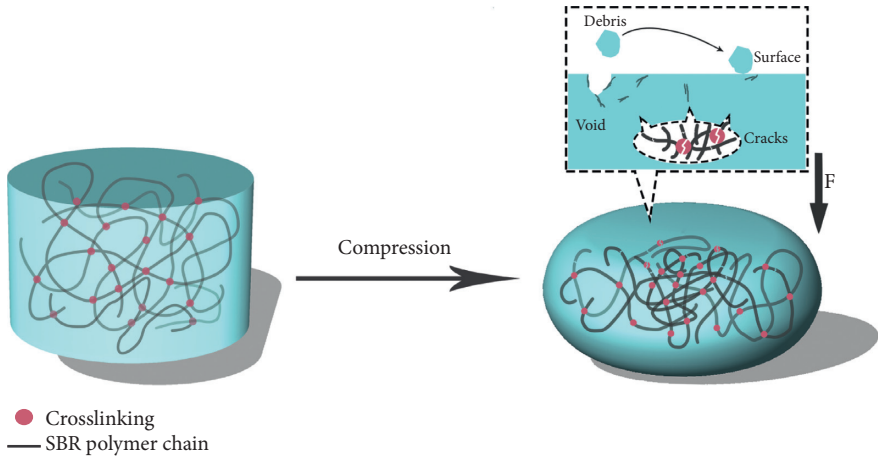

Figure 5: Characteristics of fatigue wear in rubber caused by repeated compressive stress cycles applied.

compressive creep behavior and compression set tests. The creep behavior of rubber materials is time-dependent deformation under stress as shown in Figure 6(a). The results show that initial creep strain accounts for a large proportion of the total creep strain, and the creep strain remains relatively stable during the period 500 to 3600 s. The compressive creep analysis of SBR shows that the magnitude of creep strain decreases with an increase in crosslinking density. When the samples are subjected to repeated compressive loads, the mobility of molecular chains is limited by rearrangement and orientation. The higher the crosslinking density is, the worse the molecular mobility is. In addition, the DCP-SBR samples and S-SBR samples show obviously different creep behaviors. The DCP-SBR samples have smaller creep strain than the S-SBR samples even though the crosslinking densities of DCP-SBR samples are lower than those of S-SBR 2 and S-SBR 3, implying that the DCP-SBR possesses superior creep resistance. The better creep resistance of peroxide-cured SBR is because C-C crosslink formation brings about a harder SBR, which further improves the creep resistance. The compression set offers clues about rubber's resistance to deformation under compressive stress. The trend of the compression set is similar to the creep strain curve. Figure 6(b) shows a compression set of S-SBR samples and DCP-SBR samples under the compression state. The compression set of all the samples increased with decreasing crosslinking density. As mentioned above, the elevated crosslink density limits the mobility, as the crosslinked network prevents the polymer from reaching high deformations.

These results provide evidence that peroxide-cured SBR samples possess excellent creep resistance and lower compression set at room temperature. It is ascribed to a large number of carbon-carbon linkages that have higher bond

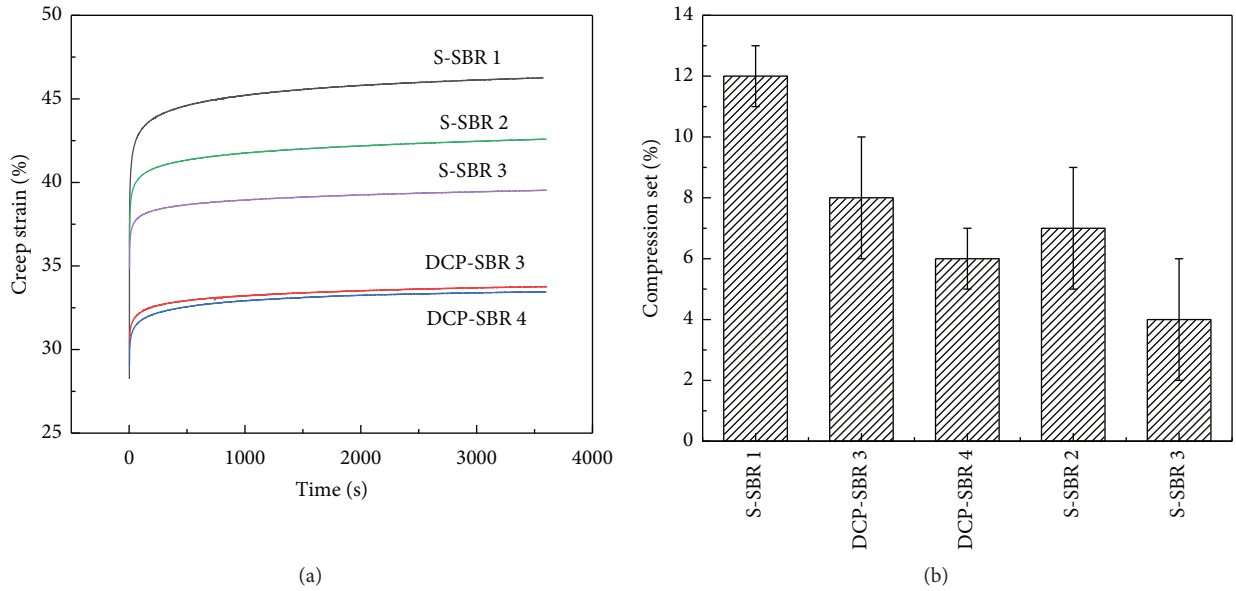

(a) (b)

Figure 6: Creep behavior (a) and compression set (b) of five samples as a function of time under compression.

energy as compared with the polysulfide linkages. This characteristic is responsible for the reduced compression set and creep deformation of DCP-SBR samples.

4. Conclusions

In this work, we prepared a series of S-SBR and DCP-SBR compounds with different sulfur and DCP loadings. The effect of network structure on compressive fatigue behavior was investigated. The main conclusions are summarized as follows:

(i) The surface damage of the two samples grows more serious as the number of compressive cycles increases. Moreover, cyclic compression caused less surface damage to S-SBR 2 than to DCP-SBR 5 under the same compressive cycles. After the compressive fatigue test, there are two main types of damage: peeling and spalling. The peeling usually shows as a wave, while the spalling shows as deeper voids on the surface.

(ii) Even if the crosslinking density of the two samples is similar, DCP-SBR 5 provides higher energy dissipation than S-SBR 2 during cyclic compression.

(iii) The creep deformation and compression set of all the samples decreased with the crosslinking density increasing. The DCP-SBR samples show smaller creep deformation and compression sets than the S-SBR samples.

Data Availability

The data used to support the findings of this study are available from the corresponding author upon request.

Conflicts of Interest

The authors declare that they have no conflicts of interest.

References

[1] W. Lou, W. Zhang, T. Jin et al., "Stress-thermal oxidative aging behavior of hydrogenated nitrile rubber seals," *Journal of Applied Polymer Science*, vol. 136, no. 7, Article ID 40714, 2018.

[2] M. F. Sonnenschein, R. Prange, and A. K. Schrock, "Mechanism for compression set of TDI polyurethane foams," *Polymer*, vol. 48, no. 2, pp. 616–623, 2007.

[3] P. Tangudom, S. Thongsang, and N. Sombatsompop, "Cure and mechanical properties and abrasive wear behavior of natural rubber, styrene-butadiene rubber and their blends reinforced with silica hybrid fillers," *Materials & Design*, vol. 53, pp. 856–864, 2014.

[4] O. Gehrmann, N. H. Kröger, M. Krause et al., "Dissipated energy density as fatigue criterion for non-relaxing tensional loadings of non-crystallizing elastomers," *Polymer Testing*, vol. 78, 2019.

[5] Q. Li, X. Huang, and W. Huang, "Fatigue property and microstructure deformation behavior of multiphase microstructure in a medium-carbon bainite steel under rolling contact condition," *International Journal of Fatigue*, vol. 125, 2019.

[6] C. M. Everitt and B. Alfredsson, "Surface initiation of rolling contact fatigue at asperities considering slip, shear limit and thermal elastohydrodynamic lubrication," *Tribology International*, vol. 137, 2019.

[7] Y. Guo, J. Wang, K. Li, and X. Ding, "Tribological properties and morphology of bimodal elastomeric nitrile butadiene rubber networks," *Materials & Design (1980–2015)*, vol. 52, pp. 861–869, 2013.

[8] H. Liang, Y. Fukahori, A. G. Thomas, and J. J. C. Busfield, "The steady state abrasion of rubber: why are the weakest rubber compounds so good in abrasion?" *Wear*, vol. 268, no. 5-6, pp. 756–762, 2010.

[9] N. Yan, H. Xia, Y. Zhan, and G. Fei, "New insights into fatigue crack growth in graphene-filled natural rubber composites by microfocus hard-x-ray beamline radiation," *Macromolecular Materials and Engineering*, vol. 298, no. 1, pp. 38–44, 2013.

[10] F. Hakami, A. Pramanik, N. Ridgway et al., "Developments of rubber material wear in conveyer belt system," *Tribology International*, vol. 111, 2017.
[11] G.-H. Lim, K. Bodjona, K. P. Raju, S. Fielding, V. Romanov, and L. Lessard, "Evolution of mechanical properties of flexible epoxy adhesives under cyclic loading and its effects on composite hybrid bolted/bonded joint design," *Composite Structures*, vol. 189, pp. 54–60, 2018.
[12] C. Nicolas, O. Oguzhan, P. D. Edith et al., "Strain-induced network chains damage in carbon black filled EPDM," *Polymer*, vol. 175, pp. 329–338, 2019.
[13] H. B. Van, D. Moens, R. Boonen et al., "On the difference in material structure and fatigue properties of nylon specimens produced by injection molding and selective laser sintering," *Polymer Testing*, vol. 32, pp. 972–981, 2013.
[14] S. Seichter, V.-M. Archodoulaki, T. Koch, A. Wondracek, and A. Holzner, "Investigation of different influences on the fatigue behaviour of industrial rubbers," *Polymer Testing*, vol. 59, pp. 99–106, 2017.
[15] Y. Zhan, N. Yan, G. Fei, H. Xia, and Y. Meng, "Crack growth resistance of natural rubber reinforced with carbon nanotubes," *Journal of Applied Polymer Science*, vol. 137, no. 10, p. 48447, 2020.
[16] F. Abraham, T. Alshuth Jerrams, and S. Jerrams, "Dependence on mean stress and stress amplitude of fatigue life of EPDM elastomers," *Plastics, Rubber and Composites*, vol. 30, no. 9, pp. 421–425, 2001.
[17] Sarina, J. Zhang, and L. Zhang, "Dynamic mechanical properties of eucommia ulmoides gum with different degree of cross-linking," *Polymer Bulletin*, vol. 68, no. 7, pp. 2021–2032, 2012.
[18] H. Samantha, P. Christopher, M. Tesfaldet, and J. P. Richard, "Experimental determination of the quantity and distribution of chemical crosslinks in unaged and aged natural rubber, part 1: peroxide vulcanization," *Polymer Testing*, vol. 70, pp. 263–274, 2018.
[19] J.-B. Le Cam, B. Huneau, and E. Verron, "Description of fatigue damage in carbon black filled natural rubber," *Fatigue & Fracture of Engineering Materials & Structures*, vol. 31, no. 12, pp. 1031–1038, 2008.
[20] B. Wu and H. Jin, "Compressive fatigue behavior of compound concrete containing demolished concrete lumps," *Construction and Building Materials*, vol. 210, pp. 140–156, 2019.
[21] C.-C. Wu and Y.-C. Chiou, "Stress-strain response of cylindrical rubber fender under monotonic and cyclic compression," *Materials*, vol. 12, no. 2, pp. 282–299, 2019.
[22] R. H. Luciana, C. R. Regina, and G. Jaqueline, "Effect of the cure system on aging resistance of natural rubber compounds," *Journal of Elastomers & Plastics*, vol. 51, pp. 1–13, 2019.
[23] X. Fu, C. Huang, Y. Zhu et al., "Characterizing the naturally occurring sacrificial bond within natural rubber," *Polymer*, vol. 161, pp. 41–48, 2019.
[24] A. Pramanik, L. C. Zhang, and J. A. Arsecularatne, "Deformation mechanisms of MMCs under indentation," *Composites Science and Technology*, vol. 68, no. 6, pp. 1304–1312, 2008.
[25] C. Wang, A. Hausberger, M. Berer, G. Pinter, F. Grün, and T. Schwarz, "An investigation of fretting behavior of thermoplastic polyurethane for mechanical seal application," *Polymer Testing*, vol. 72, pp. 271–284, 2018.